

Model Design and Simulation of an 80 kW Capacitor Coupled Substation Derived from a 132 kV Transmission Line

Sinqobile Wiseman Nene, Bolanle Tolulope Abe, Agha Francis Nnachi

Department of Electrical Engineering, Tshwane University of Technology, eMalahleni, South Africa
Email: wnene@hailienene.com, AbeBT@tut.ac.za, NnachiAF@tut.ac.za

How to cite this paper: Nene, S.W., Abe, B.T. and Nnachi, A.F. (2025) Model Design and Simulation of an 80 kW Capacitor Coupled Substation Derived from a 132 kV Transmission Line. *Open Journal of Modelling and Simulation*, 13, 1-19.

<https://doi.org/10.4236/ojmsi.2025.131001>

Received: Octobre 31, 2024

Accepted: December 13, 2024

Published: December 16, 2024

Copyright © 2025 by author(s) and Scientific Research Publishing Inc.
This work is licensed under the Creative Commons Attribution International License (CC BY 4.0).

<http://creativecommons.org/licenses/by/4.0/>



Open Access

Abstract

The global rise in energy demand, particularly in remote and sparsely populated regions, necessitates innovative and cost-effective electrical distribution solutions. Traditional Rural Electrification (RE) methods, like Conventional Rural Electrification (CRE), have proven economically unfeasible in such areas due to high infrastructure costs and low electricity demand. Consequently, Unconventional Rural Electrification (URE) technologies, such as Capacitor Coupled Substations (CCS), are gaining attention as viable alternatives. This study presents the design and simulation of an 80 kW CCS system, which taps power directly from a 132 kV transmission line to supply low-voltage consumers. The critical components of the CCS, the capacitors are calculated, then a MATLAB/Simulink model with the attained results is executed. Mathematical representation and state-space representation for maintaining the desired tapped voltage area also developed. The research further explores the feasibility and operational performance of this CCS configuration, aiming to address the challenges of rural electrification by offering a sustainable and scalable solution. The results show that the desired value of the tapped voltage can be achieved at any level of High Voltage (HV) with the selection of capacitors that are correctly rated. With an adequately designed control strategy, the research also shows that tapped voltage can be attained under both steady-state and dynamic loads. By leveraging CCS technology, the study demonstrates the potential for delivering reliable electricity to underserved areas, highlighting the system's practicality and effectiveness in overcoming the limitations of conventional distribution methods.

Keywords

Capacitor-Coupled Substation, Transmission Line-linked Capacitor-Coupled Substation, Capacitor-Coupled Substation Simulation, Microgrids, Rural

1. Introduction

The rapid growth in global energy demand, coupled with the need for sustainable and economically viable power solutions, has prompted a re-evaluation of traditional electrical distribution methods, especially in remote and sparsely populated regions [1]. The demand for efficient and cost-effective electrical distribution has driven innovations in power system architectures [2]. Traditional approaches to Rural Electrification (RE) such as Conventional Rural Electrification (CRE) have been considered economically unviable in sparsely populated regions, particularly rural areas, as they are often associated with minimal electricity demand perception [3] [4]. As a result, Un-Conventional Rural Electrification (URE) technologies are being explored to provide a cost-effective system for supplying electrical power to rural areas [5] [6]. CCS represents a technology that is currently under continuous exploration for rural electrification purposes [7] [8]. CCS entails coupling capacitors used to tap electrical power from HV lines and convert it to distribution-level voltages. However, directly tapping power from an HV transmission line using CCS can induce transient behaviours within the electrical network, inevitably impacting the primary components of the CCS [9]-[11].

This article presents a comprehensive review of a model design and simulation of an 80 kW CCS tapped from a 132 kV transmission line. The main objective of this study is to assess the feasibility and performance of the proposed CCS configuration, designed with the aim of delivering electricity directly from the HV lines to the LV consumers. Microgrids, while recognized as a potential solution, have not yet developed a comprehensive business model that effectively balances affordability with satisfactory cost recovery [12]. By using CCS, electrification to remote or sparsely populated areas can be cost-effective as opposed to using conventional distribution network infrastructure [4].

1.1. Research Problem

The increasing demand for efficient and cost-effective electrical distribution, particularly in remote and sparsely populated areas, necessitates innovative power system architectures. Conventional approaches to rural electrification, such as the use of standard distribution networks, have proven economically unviable due to the high infrastructure costs and low electricity demand in these regions. Consequently, unconventional solutions like Capacitor Coupled Substations (CCS) are being explored as potential alternatives.

This study seeks to evaluate the feasibility and performance of an 80 kW CCS design, which taps power directly from a 132 kV transmission line, to supply electricity to low-voltage consumers. By investigating this configuration, the research aims to determine whether CCS can serve as a cost-effective solution for rural

electrification, overcoming the limitations of traditional distribution methods and addressing the challenge of delivering affordable, reliable electricity to sparsely populated areas.

1.2. Contribution

The study contributes to the ongoing exploration of CCS by providing a detailed design and simulation of an 80 kW CCS system. It enhances understanding of CCS's practical applications in rural electrification, offering insights into the system's operational performance, stability, and potential as a scalable solution for delivering electricity to underserved areas.

1.3. Novelty Contribution

While CCSs have been explored theoretically, their application for direct tapping from HV lines to supply electricity to LV consumers, particularly in sparsely populated or rural areas, remains unexplored. The study provides a unique approach by proposing and simulating an 80 kW CCS system, specifically designed to deliver electricity from a 132 kV transmission line to LV consumers. This fills a gap in the existing research, where practical implementations of such systems are scarce.

2. Background Theory

One of the recent instances of practical implementation of a CCS has clearly demonstrated the system's feasibility and effectiveness in supplying electrical power to dedicated loads [13]. Through rigorous testing and operation, practical studies have shown that CCS can reliably meet the energy needs of specific consumers or applications, thereby, highlighting its potential as a viable solution for electrification in various contexts such as in sparsely populated areas or low dedicated loads [14]. A CCS can be integrated into an electrical transmission network using either a nominal- π or nominal-T configuration. The nominal-T configuration is typically employed for shorter transmission lines, extending up to 80 km, while the nominal- π configuration is preferred for medium-length transmission lines exceeding 80 km [15]. In essence, current studies do not provide any limitations on the type of transmission line where a CCS can be adopted.

Figure 1 below illustrates the simplified depiction of a typical CCS. This approach is similar to that of a Capacitive Voltage Transformer (CVT), which is a transformer commonly used in power systems to reduce extra-high voltage signals to low voltage signals for tasks such as metering or operating protective relays [16] [17].

The simplified CCS, as shown in **Figure 1** above, employs a capacitor-divider configuration where capacitors (C_1 and C_2) are linked across the incoming voltage (V_{in}) to generate the desired tap-voltage (V_T), which is measured from the tapping node located between the two capacitors. The voltage output (V_{out}) is calculated by subtracting the voltage drop across the inductor (L) from V_T . It is important to

note that C_1 and C_2 refer to capacitor banks rather than individual capacitors where C_1 represents Capacitor Bank 1, while C_2 represents Capacitor Bank 2.

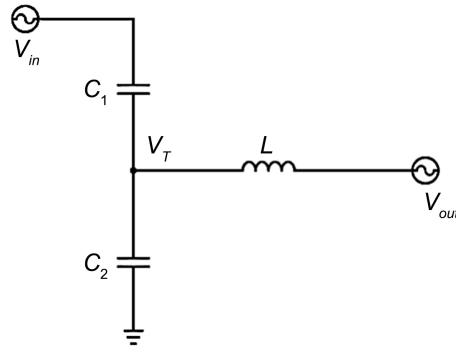


Figure 1. Overly simplified CCS [18].

The tap-voltage (V_T) is calculated as follows:

$$V_T = V_{in} \times \frac{C_1}{C_1 + C_2} \quad (1)$$

The output voltage is calculated as follows:

$$V_{out} = V_T - V_{L_1} \quad (2)$$

The output voltage can also be represented as follows:

$$V_{out} = \frac{C_1}{C_1 + C_2} \times V_L \quad (3)$$

The equations provided, as (1), (2), and (3), serve as the basis for determining the elements of a CCS. The objective is to ensure the stability of V_{out} as the CCS delivers power to a downstream transformer within the distribution network.

In **Figure 2** below, the equivalent CCS connected to a standard transmission line is depicted.

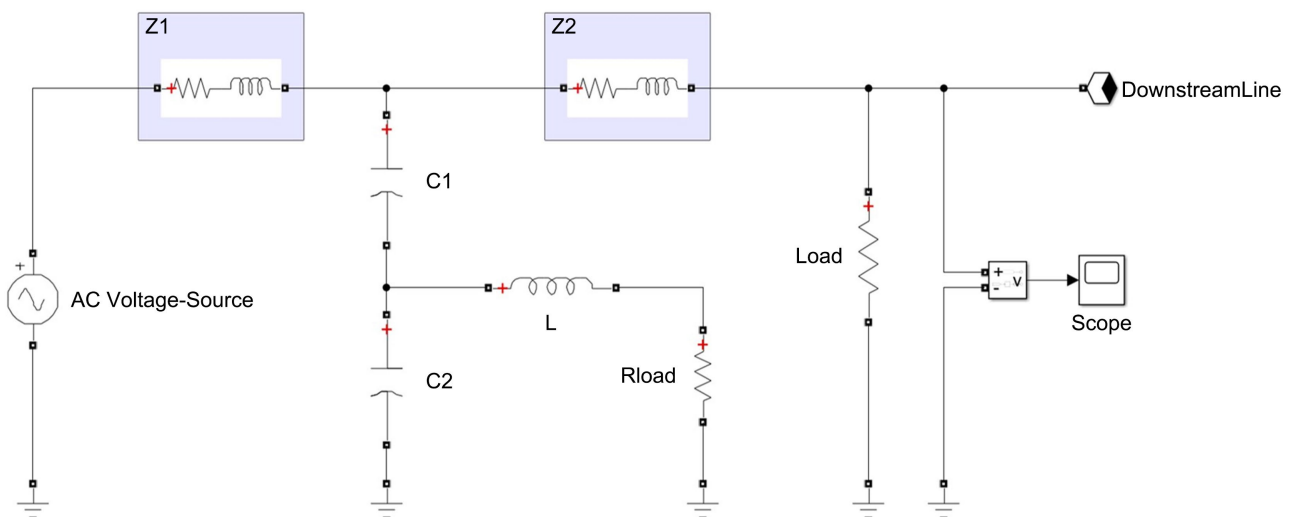


Figure 2. CCS connected to a typical transmission line.

3. Methodology

The methodology outlines the sequential steps undertaken in a research study [19]. In this study, the methodology undertaken involved the calculation of the required capacitors to achieve the desired tap voltage, the mathematical representation of the system and the development, modeling, and analysis of a CCS system using MATLAB/Simulink software. Subsequently, the results derived from the MATLAB/Simulink model were thoroughly analysed. **Figure 3** illustrates the designed block diagram model, while **Figure 4** and **Figure 5** depict the line model utilized in the analysis. These figures provide visual representations of the models employed in the study, facilitating a comprehensive understanding of the research approach and findings of the research.

Figure 3 displays the model block diagram encompassing various components, including the supply block, the transmission line segment preceding the CCS tap node, the transmission line segment succeeding the CCS tap node, the downstream transmission line block, the CCS block itself, and the CCS load block. Additionally, **Figure 4** shows the physical model representation of a CCS.

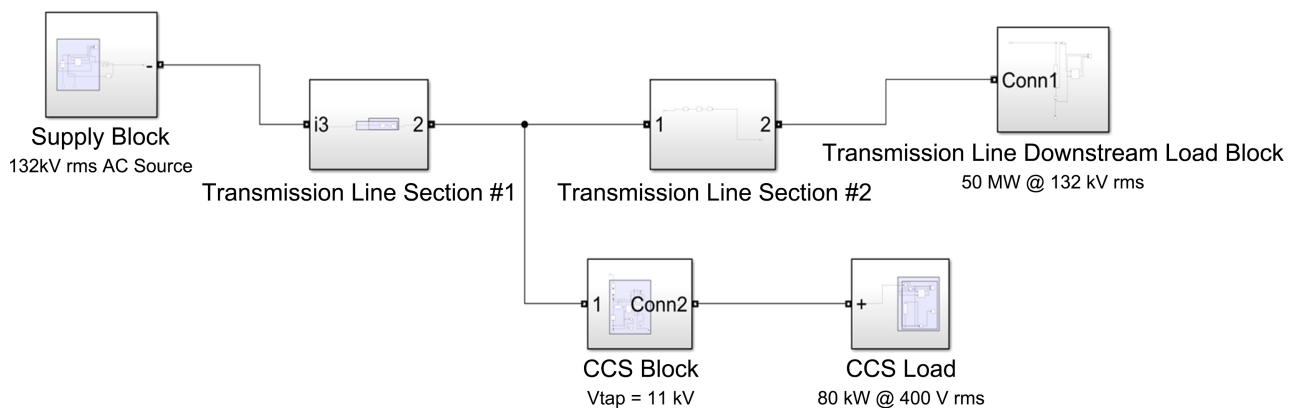


Figure 3. Model block diagram.

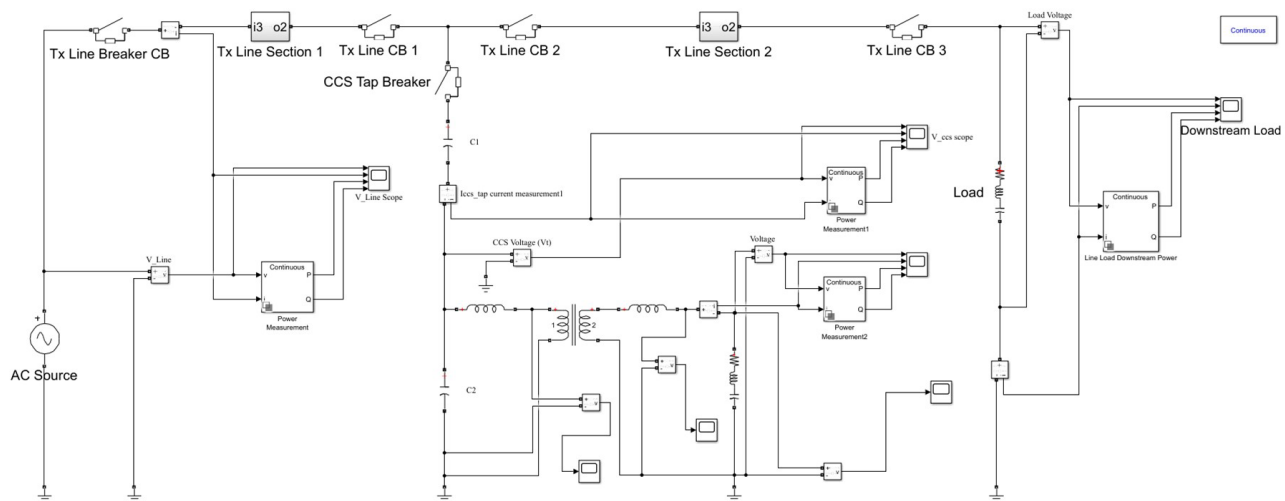


Figure 4. CCS model.

3.1. Parameters Used

The aim of this study is to develop and simulate an 80 kW loaded Capacitor Coupled Substation (CCS) connected to a standard transmission network. The selected transmission network is operated at 132 kVrms. To define the parameters of the CCS, predetermined values were used, and background calculations were conducted and the results were used for the model. The selected parameters are detailed in **Table 1**.

Table 1. Model system known parameters.

Parameter	Value	Description
V_s	132 kV rms	Supply voltage representing upstream of the transmission line
V_T	11 kV rms	The desired tap voltage for the CCS
CCS load	400 V rms, 50 Hz, 80 kW, 0.8 PF	The CCS load voltage level
Downstream load	132 kV rms, 50 Hz, 50 MW	Load downstream of the CCS tap note

The parameters in **Table 1** are used to calculate the variables required in order to achieve the desired V_{TAB} and thus, the CCS load voltage of 400 V rms. The voltage selected is based on readily available and commonly used transmission lines and distribution transmission voltages in South Africa.

Using (1), (2) and (3), with known supply voltage and the desired tap voltage, the respective capacitors C_1 and C_2 are calculated.

3.2. Modeling and Simulation

The process of modeling the system involves the utilization of MATLAB/Simulink software, a powerful computational tool widely employed in engineering research. Furthermore, to ensure a comprehensive analysis, different voltage levels were used to determine the impact on the capacitors to keep tapped voltage within acceptable tolerances. This approach provided a deeper understanding of the system's behaviour under varying conditions. The parameters used in the simulated model, crucial for accurately capturing the system behaviour, are outlined in **Table 1**.

The model utilized for simulating the system is depicted in **Figure 4** in the preceding section. This model was streamlined by employing internal MATLAB/Simulink parameters within the subsystem. The primary parameter values were extracted mainly from six model scopes, as outlined in **Table 2**.

The simulation was conducted with all circuit breakers in the system remaining closed for the entire duration of the 1.5-second simulation run. The findings from this simulation are elaborated upon in Section 4.

Table 2. Measured parameters by scope.

Scope number	Scop measured parameters
Scope 1	Supply parameters
Scope 2	Transmission network downstream parameters
Scope 3	CCS tap parameter
Scope 4	Distribution transformer primary voltage
Scope 5	Distribution transformer secondary voltage
Scope 6	CCS load parameter

4. Results and Discussion

The results obtained from the calculations and simulated model are presented in detail. The results are analysed and discussed to provide comprehensive insights into the performance of the system. These findings are visually represented, and each offers a distinct perspective on various aspects of the simulation. Through the interpretation of these figures, we aim to assess the behaviour and characteristics of the simulated system under normal steady state conditions, contributing to a deeper understanding of its functionality.

4.1. Calculated Results

Using the known parameters as per **Table 1**, to calculate the values of the capacitor banks C_1 and C_2 with the given parameters, the following results were achieved.

Using:

- $V_s = 132$ kV rms
- $V_{tap} = 11$ kV rms
- $V_{CCS-Load} = 400$ V rms
- Frequency $f = 50$ Hz
- CCS Load = 80 kW at 0.8 Power Factor
- Downstream Load = 132 kV rms, 50 MW
- Line Length = 300 km

From Equation (1), C_1 and C_2 are calculated as:

$$\frac{C_1}{C_1 + C_2} = \frac{V_{tap}}{V_s}$$

With the known supply voltage and the desired V_{tap} , the ratio is:

$$\frac{C_1}{C_1 + C_2} = \frac{11 \text{ kV}}{132 \text{ kV}} = \frac{11}{132} = \frac{1}{12}$$

Therefore, the relationship between C_1 and C_2 is:

$$C_2 = 11C_1$$

The individual capacitor banks capacitance is calculated using the system frequency of $f = 50$ Hz and the relationship between the reactance X_C and capacitance C as:

$$X_C = \frac{1}{2\pi f C}$$

Ignoring the load impedance gives the ratio of the capacitors as 1:11 (from $C_2 = 11C_1$). Therefore:

$$C_1 = \frac{C_{total}}{12} \quad \text{and} \quad C_2 = \frac{11C_{total}}{12}$$

The actual values of C_1 and C_2 , with the CCS power of 80 kW at 0.8PF is calculated from:

$$\text{Apparent Power } S = \frac{P}{PF} = \frac{80 \text{ kW}}{0.8} = 100 \text{ kV} \cdot \text{A}$$

Assuming nominal total reactive power is balanced:

$$C_{total} \approx \frac{S}{2\pi f V_{tap}^2} \approx \frac{100 \times 10^3}{2 \times 3.14146 \times (11 \times 10^3)^2} \approx 2.63 \mu\text{F}$$

Therefore:

$$C_1 \approx \frac{2.63 \mu\text{F}}{12} \approx 0.22 \mu\text{F} \quad \text{and} \quad C_2 \approx \frac{11 \times 2.63 \mu\text{F}}{12} \approx 2.41 \mu\text{F}.$$

From the calculated value of C_1 and C_2 , the simulation values used are presented in **Table 3**.

Table 3. Simulation parameters based on calculated C_1 and C_2 .

Parameter	Value	Source
V_s	132 kV rms	Selected transmission line
V_T	11 kV rms	Selected tap voltage
CCS load	400 V rms, 50 Hz, 80 kW, 0.8 PF	Selected load value
Downstream load	132 kV rms, 50 Hz, 50 MW	Selected load value
CCS transformer	11 kV/400 V	Selected transformer
C_1	0.22 μF	Calculated capacitor 1
C_2	2.41 μF	Calculated capacitor 2
L	1 mH	Line inductance
<i>Tx line section #1</i>	300 km	Selected
<i>Tx line section #2</i>	300 km	Selected

4.2. Single Line Representation

The calculated values of C_1 and C_2 are then used to simulate the system and observe its behaviour. The results obtained from the simulation are shown in **Figures 4-8** and **Figure 9**.

Figure 5 presents the supply voltage parameters with 132 kV rms as the supply and the resulting current, active power and reactive power based on the given CCS and downstream load. The downstream load parameters are also presented in **Figure 6**.

Figure 7 presents the CCS tap node with the V_{tap} being approximately 15.6 kV peak \approx 11 kV rms, with **Figure 8** representing the resulting CCS transformer secondary voltage of approximately 565 V peak \approx 400 V rms, while **Figure 9** represents the CCS load parameters with the selected 80 kW load.

The study primarily focused on three key voltage levels: the supply voltage (V_{in}), the tap voltage (V_T), and the load voltage (V_L). These voltage levels play a critical role in the operation and performance of the system under investigation.

Simulation Results Interpretation

From the simulation results, the summarised results based on the main variable of focus, V_{tap} , are expressed in **Figure 10**, **Figure 11** and **Figure 12**, where **Figure 10** and **Figure 11** present the supply, V_{tap} and transformer secondary voltages, while **Figure 12** presents the numerical representation of the peak values for the supply and V_{tap} , respectively.

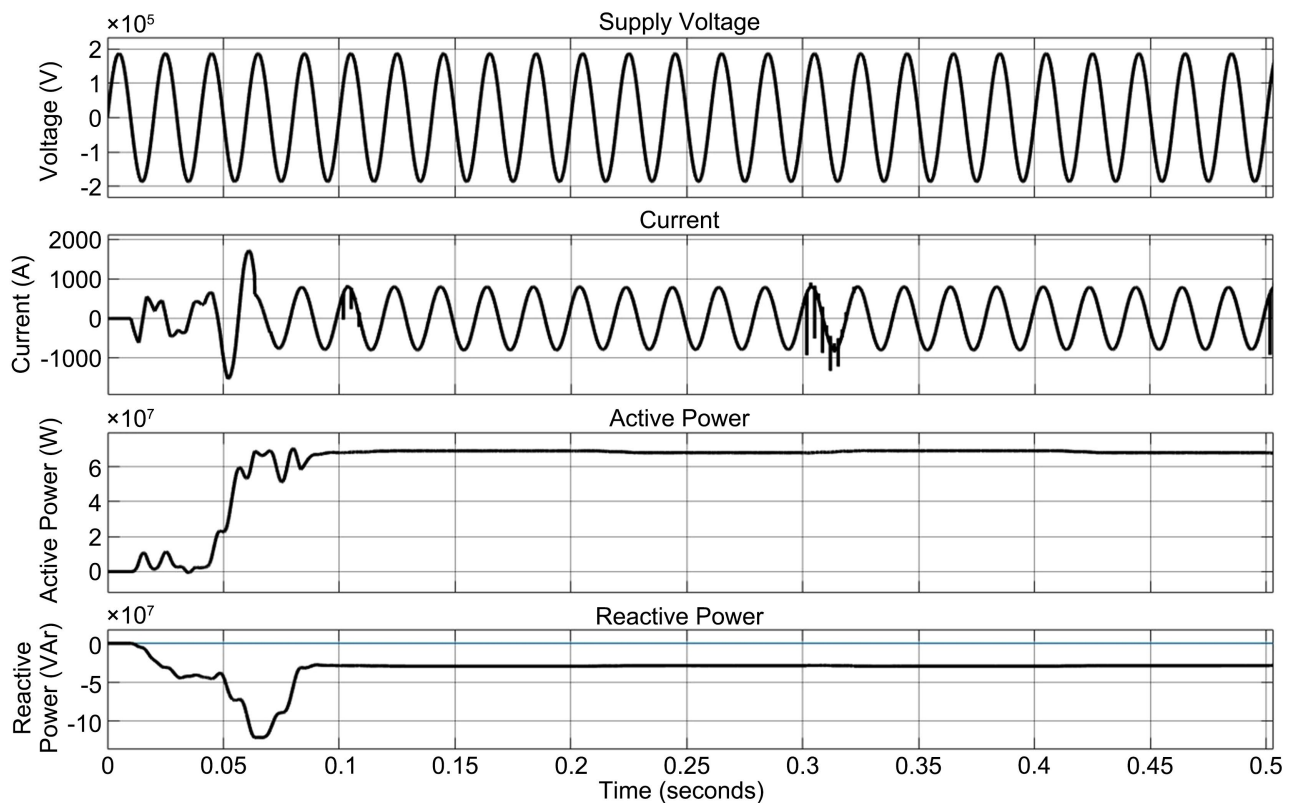


Figure 5. Supply parameters.

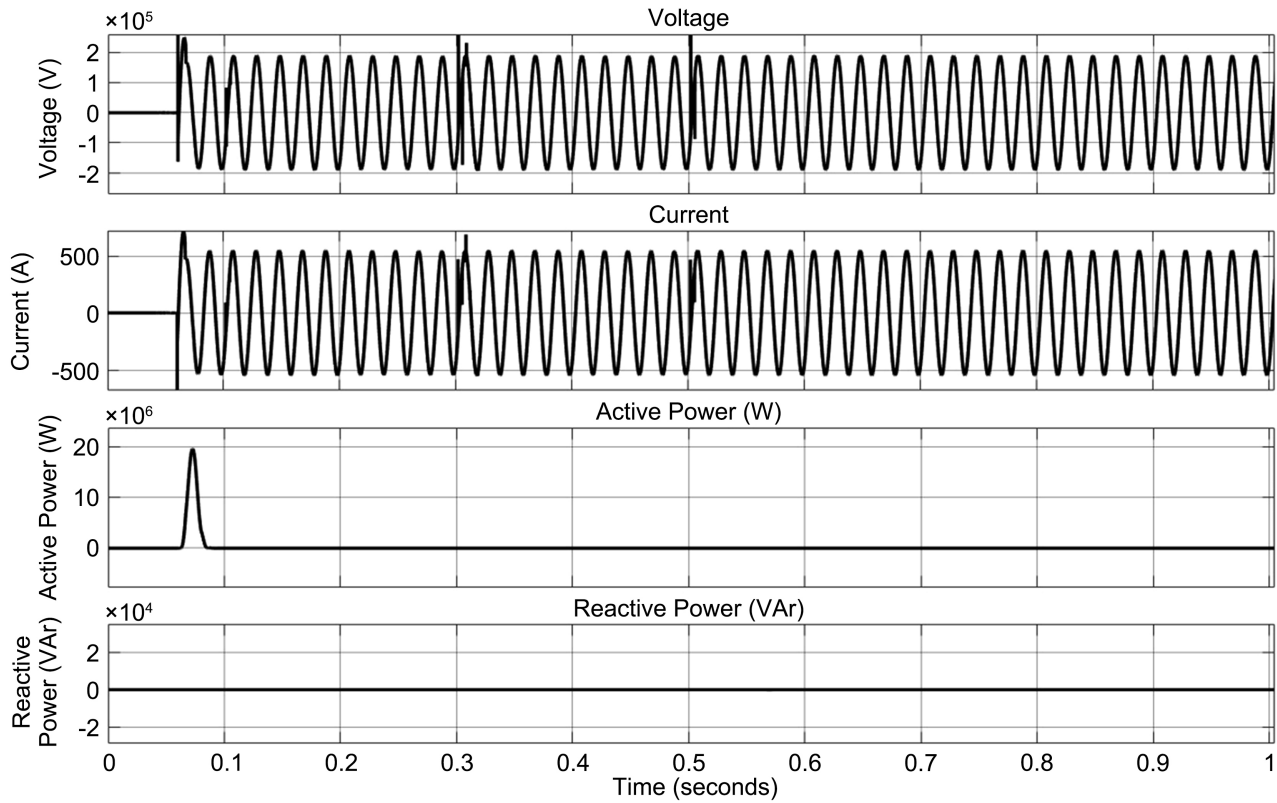


Figure 6. Downstream parameters.

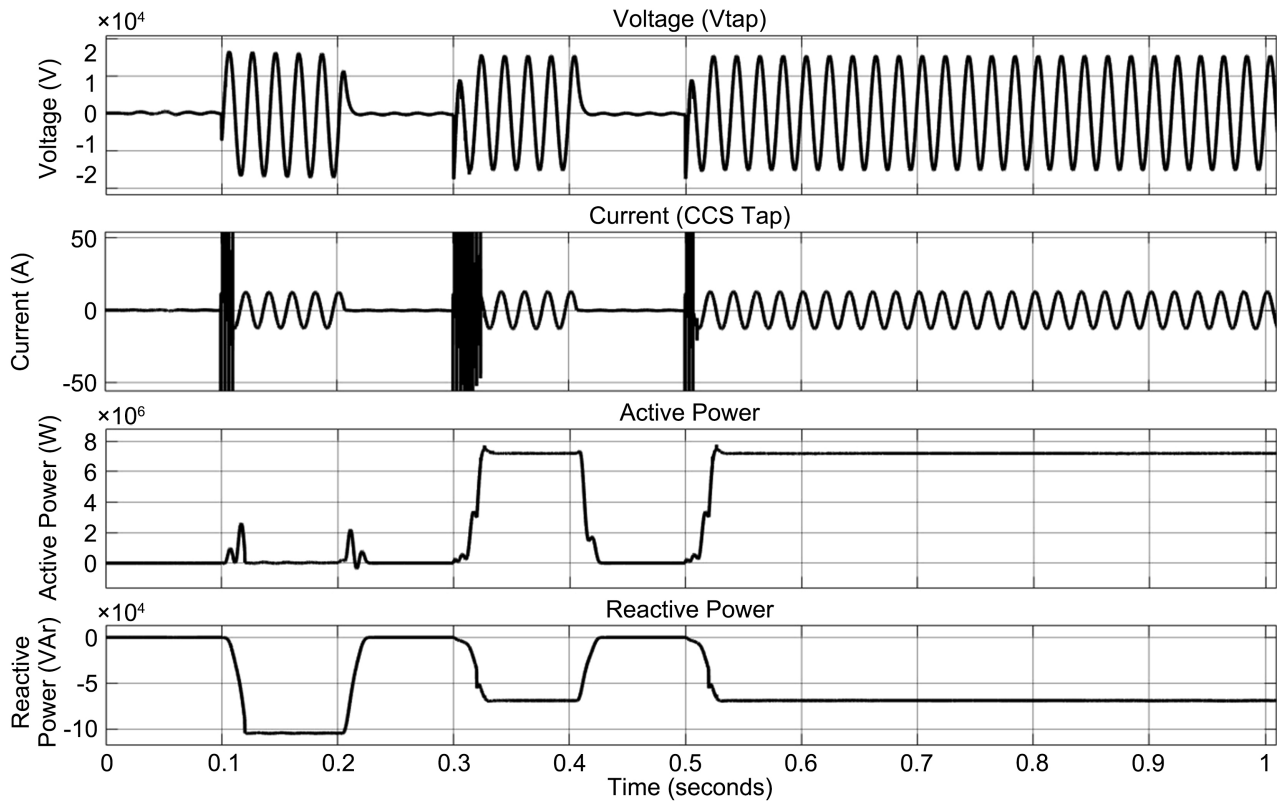


Figure 7. CCS V_{tap} node.

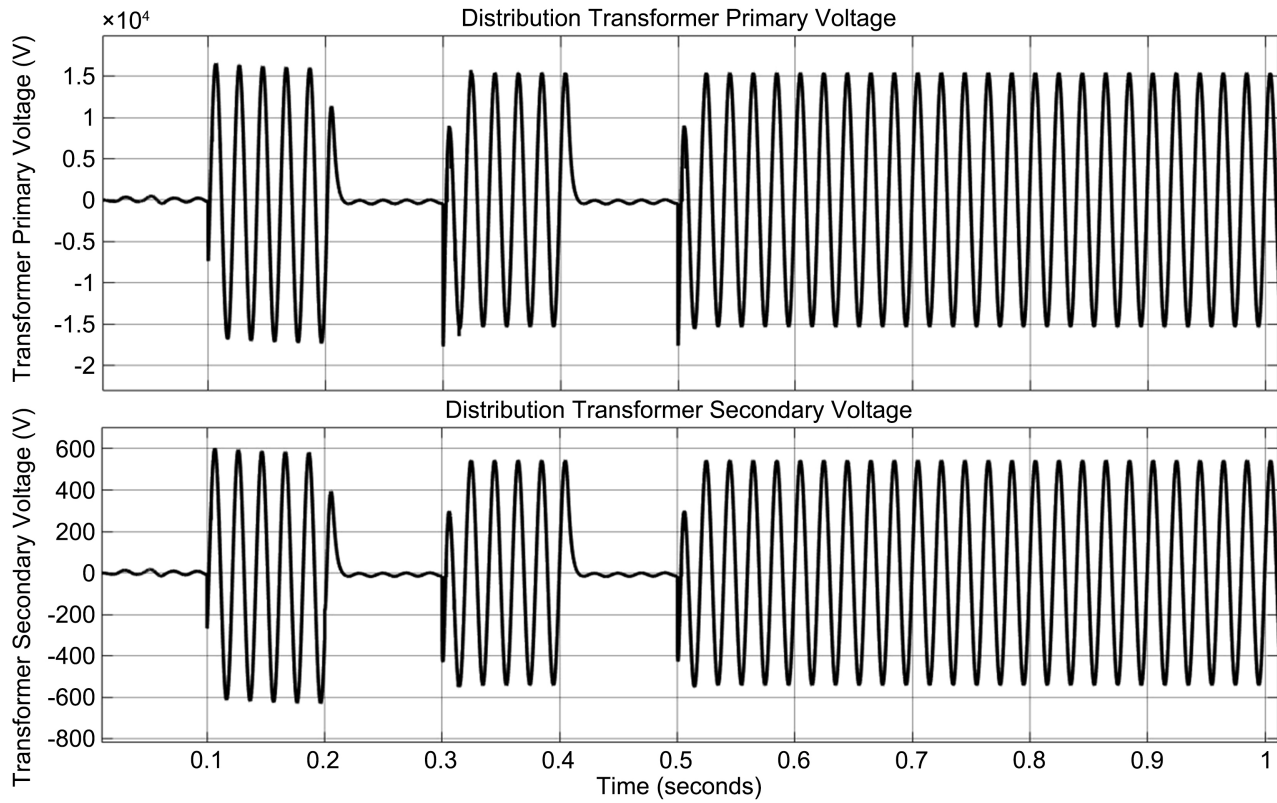


Figure 8. Distribution secondary voltage.

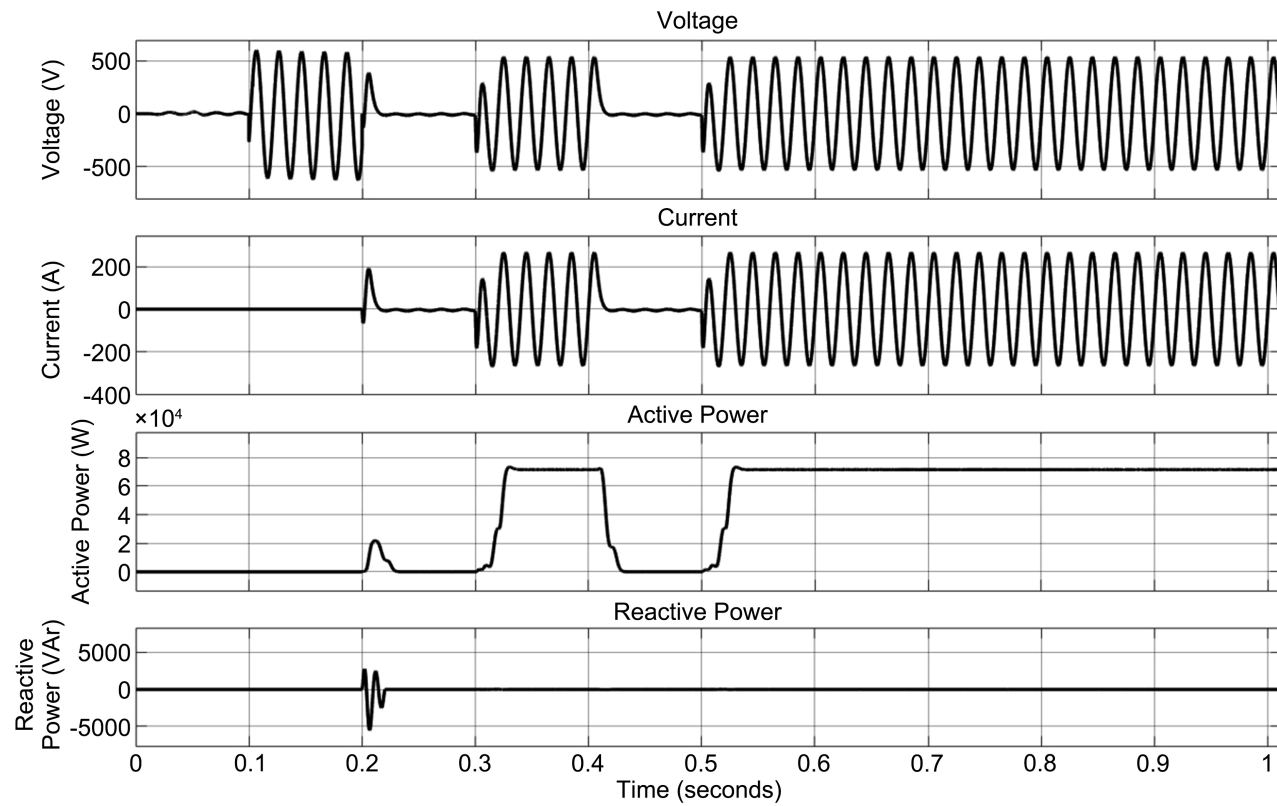


Figure 9. CCS load parameters.

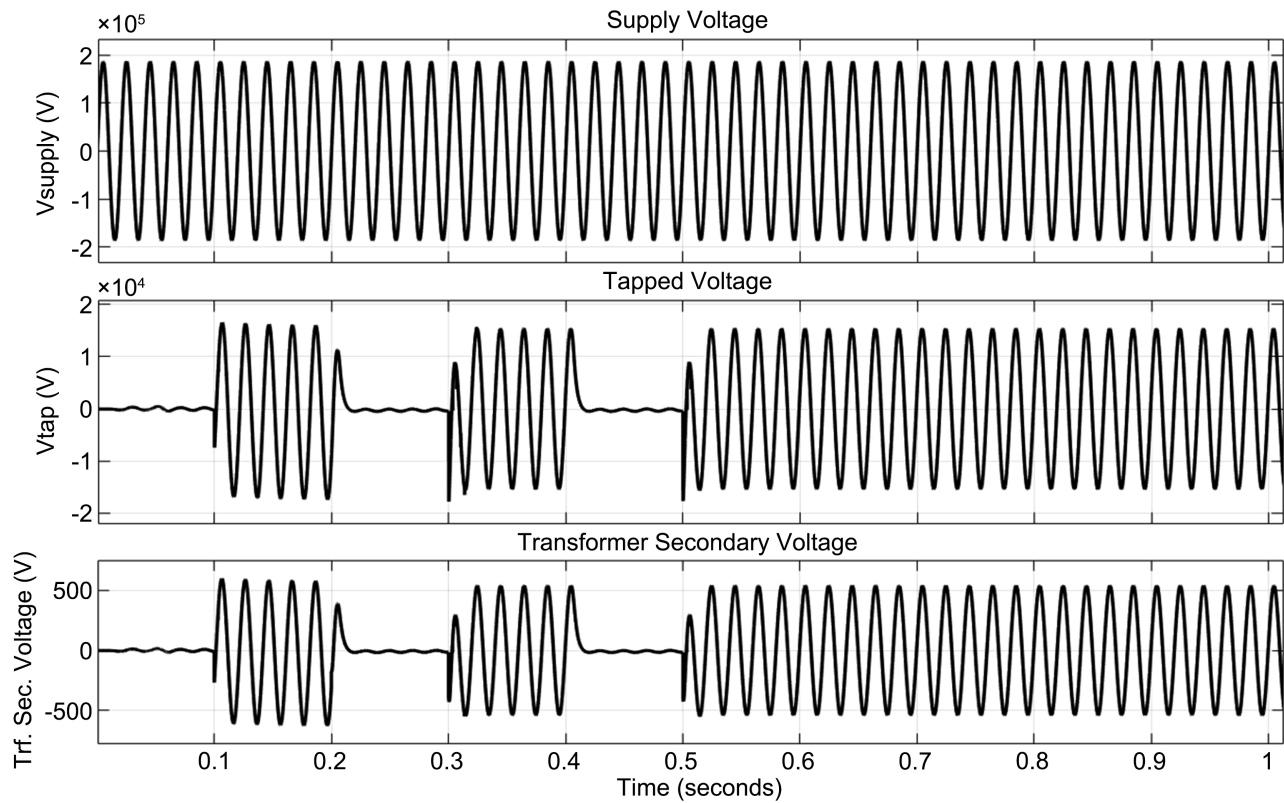


Figure 10. Supply, tapped and transformer secondary voltage.

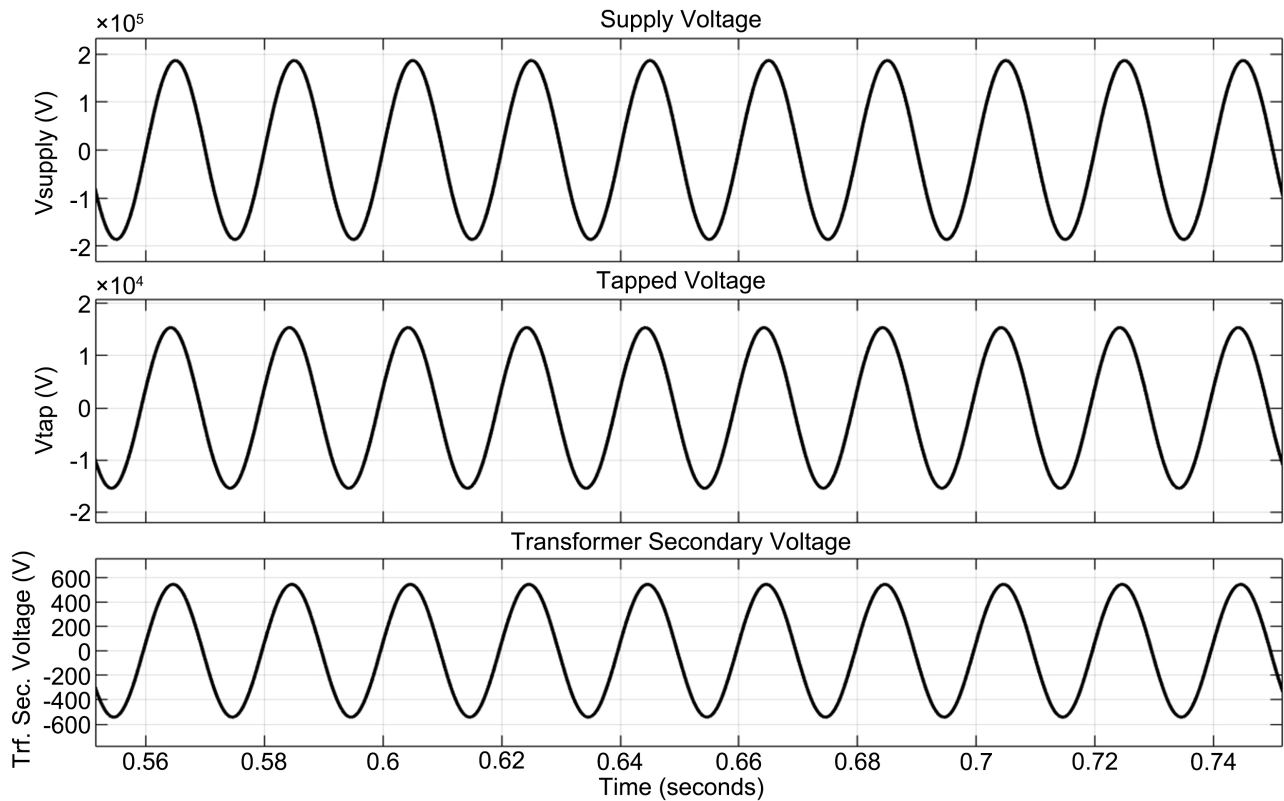


Figure 11. Supply, tapped voltage and transformer secondary voltage.

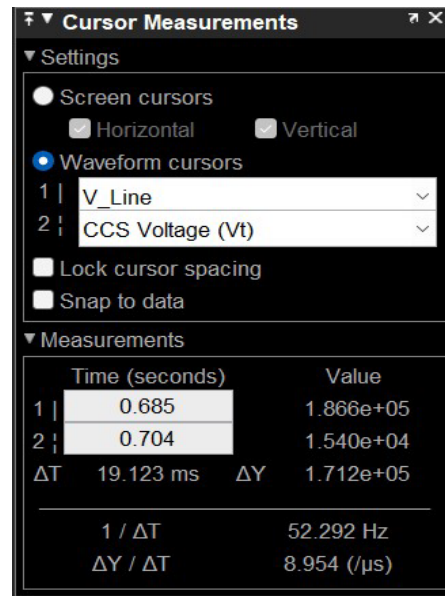


Figure 12. MATLAB measured voltage.

The measured voltages, extrapolated from **Figure 11** and **Figure 12** are:

$$V_s = V_{in} = 1.866e^{+05} = 1.866 \times 10^5 = 186.6 \text{ kV}$$

$$V_t = V_{trf, primary} = 1.540e^{+05} = 1.540 \times 10^4 = 15.4 \text{ kV}$$

Since the MATLAB results waveform represents the peak value, the root mean square (RMS) is calculated as:

$$V_{s,rms} = \frac{V_{peak}}{\sqrt{2}} = \frac{186.6 \text{ kV}}{\sqrt{2}} = 131.9 \text{ kV}$$

$$V_{t,rms} = \frac{V_{peak}}{\sqrt{2}} = \frac{15.4 \text{ kV}}{\sqrt{2}} = 10.89 \text{ kV}$$

These results show that the selected C_1 and C_2 gives the desired V_{tap} .

In **Figure 12**, V_{line} represents the incoming voltage from the voltage source supply, serving as the primary source of electrical energy. V_b or tap voltage, denotes the voltage level obtained after tapping from the transmission line, which is essential for regulating and delivering electrical power to the subsequent components of the CCS system. **Figure 12** is simplified as:

$$V_{Line} = 1.866 \times 10^5 = 186 \text{ kVpeak} = 132 \text{ kVrms}$$

$$V_{tap} = 1.540 \times 10^4 = 15.4 \text{ kVpeak} = 11 \text{ kVrms}$$

4.3. Results Repetition

The calculated results can also be used as the basis for any CCS design. The V_{tap} can be achieved by adjusting C_1 and C_2 from any HV supply. A basic MATLAB Code that can be used is presented in **Table 4**.

Table 4. MATLAB code.

```

% Define parameters
Vs = 132e3;           % Supply voltage (V)
VT_desired = 11e3;    % Desired tap voltage (V)
CCS_Load_V = 400;     % CCS load voltage (V)
f = 50;               % Frequency (Hz)
P_load = 80e3;         % Load power (W)
PF = 0.8;              % Power factor
L = 1e-3;              % Line inductance (H)
C1_initial = 0.22e-6; % Initial C1 (F)
C2_initial = 2.41e-6; % Initial C2 (F)
tolerance = 1e-3;      % Tolerance for voltage adjustment
max_iterations = 100; % Maximum iterations for adjustment

% Initial values
C1 = C1_initial;
C2 = C2_initial;

% Function to compute tap voltage VT
computeVT = @(C1, C2, Vs) Vs * C1 / (C1 + C2);

% Iterative adjustment of C1 and C2
for iter = 1:max_iterations
% Calculate current tap voltage
VT_current = computeVT(C1, C2, Vs);

% Check if VT_current is within the desired tolerance
if abs(VT_current - VT_desired) <= tolerance
break;
end

% Adjust C1 and C2 based on the difference
if VT_current < VT_desired
C1 = C1 * 1.01; % Increase C1 slightly
C2 = C2 * 0.99; % Decrease C2 slightly
else
C1 = C1 * 0.99; % Decrease C1 slightly
C2 = C2 * 1.01; % Increase C2 slightly
end
end

% Output the final values of C1 and C2
fprintf('Final C1: %.6f  $\mu$ F\n', C1 * 1e6);
fprintf('Final C2: %.6f  $\mu$ F\n', C2 * 1e6);
fprintf('Final Tap Voltage: %.2f V\n', VT_current);
fprintf('Iterations: %d\n', iter);

if iter == max_iterations
disp('Maximum iterations reached. Consider revising the tolerance
or initial conditions.');
```

The results of the code in **Table 4** are presented in **Table 5**.

The same code can be used when the supply voltage changes, as shown in the example result presented in **Table 6**, when the supply voltage is changed to 400 kV.

Testing the code on the nominal HV levels used in South Africa [20], the code can adjust C_1 and C_2 to achieve the desired tapped voltage as shown in **Table 7**.

Table 5. Table 4 MATLAB code run results.

Final C1: 0.218903 μF
 Final C2: 2.397979 μF
 Final tap voltage: 10841.13 V
 Iterations: 100

Table 6. Table 4 MATLAB code run results when V_s is 400 kV rms.

Final C1: 0.122561 μF
 Final C2: 4.282966 μF
 Final tap voltage: 10913.58 V
 Iterations: 100

Table 7. Achieved V_{tap} from different V_s .

HV Level	88 kV	132 kV	275 kV	400 kV	765 kV
C_1	0.273 μF	0.219 μF	0.147 μF	0.123 μF	0.087 μF
C_2	1.924 μF	2.398 μF	3.577 μF	4.283 μF	6.017 μF
V_{tap}	11.1 kV	10.8 kV	11.0 kV	10.9 kV	11.2 kV

Table 7 presents the resulting V_{tap} tapped from different values of V_s with C_1 and C_2 that gives that resulting V_{tap} .

4.3.1. Maintaining the Tapped Voltage Under Load

The tapped voltage (V_{tap}) can be influenced by the load [21]. V_{tap} on a steady-state circuit is derived by Equation (1). However, when the load connected changes, it affects the impedance seen by the capacitors, thus altering the V_{tap} . The load introduces an additional impedance parallel with C_2 and can be represented by Z_{C2} . If Z_L is the impedance of the load, then the effective impedance across C_2 and the load is given by:

$$Z_{eff} = \left(\frac{1}{Z_{C2}} + \frac{1}{Z_L} \right)^{-1}$$

$$\text{where: } Z_{C2} = \frac{1}{j\omega C_2} = \frac{1}{j2\pi f C_2}$$

The V_{tap} under varying load is thus derived from:

$$V_{tap} = V_s \times \frac{Z_{eff}}{Z_{eff} + Z_{C1}} \rightarrow V_{tap} = V_s \times \frac{\frac{1}{j\omega C_2} \times Z_L}{\frac{1}{j\omega C_2} + Z_L + \frac{1}{j\omega C_1}}$$

In order to maintain the desired value of V_{tap} :

- If V_{tap} is lower than desired, increase C_1 or decrease C_2
- If V_{tap} is higher than desired, decrease C_1 or increase C_2

4.3.2. Computing V_{tap} Under Dynamic Load Conditions Using State-Space Representation

Using the data from **Table 4**, a state-space representation for maintaining the desired tapped voltage (V_{tap}) on a CCS under dynamic loads can be modelled as follows, using state variables:

- $x_1(t) = V_{C1}(t)$: Voltage across capacitor C_1
- $x_2(t) = I_L(t)$: Current through the inductor L
- $x_3(t) = V_{C2}(t)$: Voltage across capacitor C_2

The state-space equations is therefore defined using Kirchhoff's Current Law (KCL) at the C_1 , with $I_s(t)$, being the current from the source, as:

$$C_1 \frac{dV_{C1}(t)}{dt} = I_s(t) - I_L(t)$$

Using Kirchhoff's Voltage Law (KVL) across L , gives:

$$L \frac{dI_L(t)}{dt} = V_{C1}(t) - V_{C2}(t)$$

While using KCL at C_2 , where $I_{load}(t)$ is the current drawn by the dynamic load connected to the system, gives:

$$C_2 \frac{dV_{C2}(t)}{dt} = I_L(t) - I_{load}(t)$$

The state-space equations are thus given as:

$$\dot{x}_1(t) = \frac{1}{C_1} (I_s(t) - x_2(t))$$

$$\dot{x}_2(t) = \frac{1}{L} (x_1(t) - x_3(t))$$

$$\dot{x}_3(t) = \frac{1}{C_2} (x_2(t) - I_{load}(t))$$

The matrix representation is thus:

$$\begin{pmatrix} \dot{x}_1(t) \\ \dot{x}_2(t) \\ \dot{x}_3(t) \end{pmatrix} = \begin{pmatrix} 0 & -\frac{1}{C_1} & 0 \\ \frac{1}{L} & 0 & -\frac{1}{L} \\ 0 & \frac{1}{C_2} & 0 \end{pmatrix} \begin{pmatrix} x_1(t) \\ x_2(t) \\ x_3(t) \end{pmatrix} + \begin{pmatrix} \frac{1}{C_1} \\ 0 \\ 0 \end{pmatrix} I_s(t) + \begin{pmatrix} 0 \\ 0 \\ -\frac{1}{C_2} \end{pmatrix} I_{load}(t)$$

The output equation, which relates the state variables to $V_{tap} = x_3(t)$, is:

$$y(t) = \begin{pmatrix} 0 & 0 & 1 \end{pmatrix} \begin{pmatrix} x_1(t) \\ x_2(t) \\ x_3(t) \end{pmatrix}$$

In order to maintain the desired V_{tap} , control input $u(t)$ is introduced as part of $I_s(t)$, making $I_s(t)$ a function of $u(t)$. The input vector B and control law can be modified accordingly to achieve the desired V_{tap} . The state-space model to use when designing control strategies to maintain the desired V_{tap}

under varying load conditions is given by:

$$\begin{aligned}\dot{x}_1(t) &= A_x(t) + B_u(t) + B_{load}I_{load}(t) \\ y(t) &= C_x(t)\end{aligned}$$

where:

$$A = \begin{pmatrix} 0 & -\frac{1}{C_1} & 0 \\ \frac{1}{L} & 0 & -\frac{1}{L} \\ 0 & \frac{1}{C_2} & 0 \end{pmatrix}, \quad B = \begin{pmatrix} \frac{1}{C_2} \\ 0 \\ 0 \end{pmatrix}, \quad B_{load} = \begin{pmatrix} 0 \\ 0 \\ -\frac{1}{C_2} \end{pmatrix}, \quad C = \begin{pmatrix} 0 & 0 & 1 \end{pmatrix}$$

The control law may include load compensation to counteract the effects of $B_{load}I_{load}(t)$. Under varying I_{load} , in order to achieve and maintain the desired V_{tap} , a gain matrix K can be designed to fulfil the control law with feedback controller $u(t) = Kx(t)$.

5. Conclusions

This study explored the feasibility and performance of an 80 kW Capacitor Coupled Substation (CCS) system tapped from a 132 kV transmission line, with the goal of providing an alternative solution for rural electrification. By integrating the CCS directly into the high-voltage network and tapping power for low-voltage consumers, the model successfully demonstrated that stable tap voltages could be achieved under varying supply conditions. The research highlights the potential of CCS technology to serve as a scalable alternative to traditional distribution networks, especially in sparsely populated regions where conventional electrification methods are economically unviable.

The simulation results revealed that the proposed CCS system could maintain the desired tap voltage even under different load conditions, provided appropriate adjustments were made to the capacitor banks. The MATLAB/Simulink model, validated through extensive calculations, confirmed that the CCS design could reliably deliver electricity to low-voltage consumers. This approach not only fills a critical gap in rural electrification research but also opens avenues for further development and practical implementation of CCS systems in remote areas.

The study contributes valuable insights into the practical application of CCS technology for rural electrification, offering a promising solution to address the challenges of delivering reliable electricity to underserved communities. Future research could build upon these findings by exploring the long-term stability, economic viability, and potential integration of renewable energy sources within the CCS framework.

Recommendations

The following is the recommendation for future research:

Further analysis of a CCS in a dynamic state is to be conducted in order to identify operability of a CCS in a real-world environment.

Conflicts of Interest

The authors declare no conflicts of interest regarding the publication of this paper.

References

- [1] Bayliss, K. and Pollen, G. (2021) The Power Paradigm in Practice: A Critical Review of Developments in the Zambian Electricity Sector. *World Development*, **140**, Article ID: 105358. <https://doi.org/10.1016/j.worlddev.2020.105358>
- [2] Samad, T. and Annaswamy, A.M. (2017) Controls for Smart Grids: Architectures and Applications. *Proceedings of the IEEE*, **105**, 2244-2261. <https://doi.org/10.1109/jproc.2017.2707326>
- [3] Falchetta, G., Pachauri, S., Byers, E., Danylo, O. and Parkinson, S.C. (2020) Satellite Observations Reveal Inequalities in the Progress and Effectiveness of Recent Electrification in Sub-Saharan Africa. *One Earth*, **2**, 364-379. <https://doi.org/10.1016/j.oneear.2020.03.007>
- [4] Saulo, M.J. (2014) Penetration Level of Un-Conventional Rural Electrification Technologies on Power Networks. Ph.D. Thesis, University of Cape Town.
- [5] Olówósejéjé, S., Leahy, P. and Morrison, A.P. (2020) A Practical Approach for Increased Electrification, Lower Emissions and Lower Energy Costs in Africa. *Sustainable Futures*, **2**, Article ID: 100022. <https://doi.org/10.1016/j.sfr.2020.100022>
- [6] Nene, S.W., Abe, B.T. and Nnachi, A.F. (2023) Modeling and Analysis of Multiple Capacitor Coupled Substations at Different Proximities. 2023 31st Southern African Universities Power Engineering Conference (SAUPEC), Johannesburg, 24-26 January 2023, 1-6. <https://doi.org/10.1109/saupec57889.2023.10057698>
- [7] Saulo, M.J. and Gaunt, C.T. (2015) The Impact of Capacitor Coupled Sub-Station in Rural Electrification of Sub-Saharan Africa. *International Journal of Energy and Power Engineering*, **4**, 12-29.
- [8] Raphalalani, T., Ijumba, N. and Jimoh, A. (2002) Capacitive Divider System for Feeding a Distribution Network from EHV Line. *PowerCon 2000. 2000 International Conference on Power System Technology. Proceedings (Cat. No.00EX409)*, Perth, 4-7 December 2000, 299-304.
- [9] Abbasi, A., Fathi, S.H. and Mihankhah, A. (2017) Elimination of Chaotic Ferroresonant Oscillations Originated from TCSC in the Capacitor Voltage Transformer. *IETE Journal of Research*, **64**, 354-366. <https://doi.org/10.1080/03772063.2017.1353928>
- [10] Radmanesh, H. (2012) Ferroresonance Elimination in 275kv Substation. *Electrical and Electronic Engineering*, **2**, 54-59. <https://doi.org/10.5923/j.eee.20120202.10>
- [11] Rojas, R.E., Chaves, J.S. and Tavares, M.C. (2023) Ferroresonance Mitigation for the Unconventional Rural Electrification System. *Electric Power Systems Research*, **223**, Article ID: 109590. <https://doi.org/10.1016/j.epsr.2023.109590>
- [12] Ogeya, M., Muhoza, C. and Johnson, O.W. (2021) Integrating User Experiences into Mini-Grid Business Model Design in Rural Tanzania. *Energy for Sustainable Development*, **62**, 101-112. <https://doi.org/10.1016/j.esd.2021.03.011>
- [13] Schilder, M., Britten, A., Mathebula, M. and Singh, A. (2005) Eskom Experience with On-Site Field Tests of a Capacitive Coupled Substation. 2005 *IEEE Power Engineering Society Inaugural Conference and Exposition in Africa*, Durban, 11-15 July 2005,

105-110.

- [14] Reeves, K., Gaunt, C.T. and Braae, M. (2011) Modelling and Dynamic Systems Analysis of Instability in a Capacitor-Coupled Substation Supplying an Induction Motor. *Electric Power Systems Research*, **81**, 888-893.
<https://doi.org/10.1016/j.epsr.2010.11.026>
- [15] Ritzmann, D., Wright, P.S., Holderbaum, W. and Potter, B. (2016) A Method for Accurate Transmission Line Impedance Parameter Estimation. *IEEE Transactions on Instrumentation and Measurement*, **65**, 2204-2213.
<https://doi.org/10.1109/tim.2016.2556920>
- [16] Mohan, V., Poornima, S. and Sugumaran, C.P. (2019) Mitigation of Ferroresonance in Capacitive Voltage Transformer Using Memelements. 2019 *International Conference on High Voltage Engineering and Technology (ICHVET)*, Hyderabad, 7-8 February 2019, 1-5. <https://doi.org/10.1109/ichvet.2019.8724375>
- [17] Chen, B., Du, L., Liu, K., Chen, X., Zhang, F. and Yang, F. (2017) Measurement Error Estimation for Capacitive Voltage Transformer by Insulation Parameters. *Energies*, **10**, Article 357. <https://doi.org/10.3390/en10030357>
- [18] de Andrade Reis, R.L., Neves, W.L.A., Lopes, F.V. and Fernandes, D. (2019) Coupling Capacitor Voltage Transformers Models and Impacts on Electric Power Systems: A Review. *IEEE Transactions on Power Delivery*, **34**, 1874-1884.
<https://doi.org/10.1109/tpwrd.2019.2908390>
- [19] Mishra, D.S.B. and Alok, D.S. (2022) Fundamentals of Research. In: Mishra, D.S.B. and Alok, D.S., Ed., *Handbook of Research Methodology*, Educreation Publishing, 2.
- [20] Buraimoh, E., Adebisi, A.A., Ayamolowo, O.J. and Davidson, I.E. (2020) South Africa Electricity Supply System: The Past, Present and the Future. 2020 *IEEE PES/IAS PowerAfrica*, Nairobi, 25-28 August 2020, 1-5.
<https://doi.org/10.1109/powerafrica49420.2020.9219923>
- [21] Pratama, N.A. and Rahmawati, Y. (2020) Evaluation of Unbalanced Load Impacts on Distribution. *Frontier Energy System and Power Engineering*, **2**, 28-35.